JOURNAL OF GEOPHYSICAL RESEARCH, VOL. 103, NO. A12, PAGES 29,169-29,181, DECEMBER 1, 1998

Physical mechanism and statistics of occurrence of an additional layer in the equatorial ionosphere

N. Balan,[1] I. S. Batista, and M. A. Abdu
Instituto Nacional de Pesquisas Espaciais, Sao Jose Dos Campos, Brazil

J. MacDougall
Department of Electrical Engineering, University of Western Ontario, London, Ontario, Canada

G. J. Bailey
Department of Applied Mathematics, University of Sheffield, Sheffield, England

Abstract. A physical mechanism and the location and latitudinal extent of an additional layer, called the F_3 layer, that exists in the equatorial ionosphere are presented. A statistical analysis of the occurrence of the layer recorded at the equatorial station Fortaleza (4°S, 38°W; dip 9°S) in Brazil is also presented. The F_3 layer forms during the morning-noon period in that equatorial region where the combined effect of the upward $\mathbf{E}\times\mathbf{B}$ drift and neutral wind provides a vertically upward plasma drift velocity at altitudes near and above the F_2 peak. This velocity causes the F_2 peak to drift upward and form the F_3 layer while the normal F_2 layer develops at lower altitudes through the usual photochemical and dynamical effects of the equatorial region. The peak electron density of the F_3 layer can exceed that of the F_2 layer. The F_3 layer is predicted to be distinct on the summer side of the geomagnetic equator during periods of low solar activity and to become less distinct as the solar activity increases. Ionograms recorded at Fortaleza in 1995 show the existence of an F_3 layer on 49% of the days, with the occurrence being most frequent (75%) and distinct in summer, as expected. During summer the layer occurs earlier and lasts longer compared to the other seasons; on the average, the layer occurs at around 0930 LT and lasts for about 3 hours. The altitude of the layer is also high in summer, with the mean peak virtual height being about 570 km. However, the critical frequency of the layer (f_oF_3) exceeds that of the F_2 layer (f_oF_2) by the largest amounts in winter and equinox; f_oF_3 exceeds f_oF_2 by a yearly average of about 1.3 MHz.

1. Introduction

The low-latitude ionosphere is known to exhibit unique features in the distribution of plasma density, temperature, and velocity which arise from the horizontal orientation of the geomagnetic field at the geomagnetic equator. In plasma density the ionosphere exhibits the well-known equatorial ionization anomaly (EIA), which is characterized by an ionization trough at the magnetic equator and crests on either side at latitudes around ±16° [*Appleton*, 1946]. Numerous experimental and modeling studies have been used to understand various aspects of the anomaly. Recently, optical techniques have been used to map the movement of the anomaly crests [*Sridharan et al.*, 1993]. Review articles have been presented by *Rajaram* [1977], *Moffett* [1979], *Anderson* [1981], *Walker* [1981], *Sastri* [1990], *Stening* [1992], *Abdu* [1997], and *Bailey et al.* [1997]. The cause of the anomaly (EIA) is well understood; it is caused by the equatorial plasma fountain that transfers ionization from around the equator to higher latitudes [*Hanson and Moffett*, 1966].

The sudden strengthening of the plasma fountain during evening hours and the subsequent nighttime cooling of the plasma give rise to a recently observed feature in the latitudinal distribution of the plasma temperature, the equatorial plasma temperature anomaly (EPTA) [*Oyama et al.*, 1997; *Balan et al.*, 1997a]. The EPTA, first revealed by observations made by the electron temperature probe on board the Hinotori satellite, has features similar to the ionization anomaly (EIA)

[1] On leave from Department of Physics, University of Kerala, Trivandrum, India.

Paper number 98JA02823.
0148-0227/98/98JA-02823$09.00

but exists only in the topside ionosphere and during the evening-midnight period. Plasma bubbles and spread F [*Booker and Wells*, 1938; *Woodman and La Hoz*, 1976] also originate in the bottomside of the evening intense plasma fountain [*Ossakow*, 1981; *Abdu et al.*, 1982; *Kelley*, 1985; *Jayachandran et al.*, 1993; *Sekar et al.*, 1994].

The purpose of the present paper is to report on a physical mechanism and the statistics of occurrence of an additional layer at equatorial latitudes. The additional layer, predicted by modeling studies, was originally called the G layer [*Balan and Bailey*, 1995]. It was later renamed the F_3 layer [*Balan et al.*, 1997b; *Jenkins et al.*, 1997] to be consistent with the well-established nomenclature of using capital letters to denote different regions of the ionosphere, for example, D, E, and F, and using the region letter followed by a number to denote distinct ionized layers within the region, for example, $F1$ and $F2$. The F_3 layer was predicted to form during the morning-noon period at altitudes above the F_2 peak; its peak density can exceed the peak density of the F_2 layer. Following the prediction, the layer was detected in ionograms recorded at the equatorial station Fortaleza (4°S, 38°W; dip 9°S) in Brazil [*Balan et al.*, 1997b]. *Jenkins et al.* [1997] presented and discussed two cases of an F_3 layer recorded at Fortaleza when there was no trace of an F_3 layer in the ionograms recorded at the nearby ionosonde station São Luis (2.3°S, 44°W; dip 0.5°S).

Although the F_3 layer has been predicted to arise from the vertical $\mathbf{E}\times\mathbf{B}$ drift at the geomagnetic equator and to be modulated by neutral wind [*Balan and Bailey*, 1995], a physical mechanism for the formation of the layer has yet to be given. In section 3 of the present paper are presented a physical mechanism and the results of a modeling study to determine the location and latitudinal extent of the layer. The proposed mechanism holds for all longitudes, while the location and latitudinal extent refer to the longitude of Fortaleza (38°W). The statistics of occurrence of the layer recorded at Fortaleza are presented in section 4. A summary of the results of this study is presented in Section 5. No attempt has been made to reproduce the observations as the $\mathbf{E}\times\mathbf{B}$ drift, and neutral wind velocities that cause the F_3 layer were not measured.

2. Model Calculations

The model calculations were carried out for the longitude of Fortaleza using SUPIM [*Bailey and Balan*, 1996; *Bailey et al.*, 1997]. In SUPIM, coupled time-dependent equations of continuity, momentum, and energy balance for the O^+, H^+, He^+, N_2^+, O_2^+, and NO^+ ions, and the electrons, are solved along closed dipole magnetic field lines between altitudes of about 130 km in conjugate hemispheres to give values for the concentrations, field-aligned fluxes, and temperatures of the ions and electrons at a discrete set of points along the field lines. For the present study, the model equations are solved along 114 eccentric-dipole magnetic field lines distributed with apex altitude between 150 and 5000 km and with the number of points along the field lines increasing with apex altitude from 201 to 301; this gives a

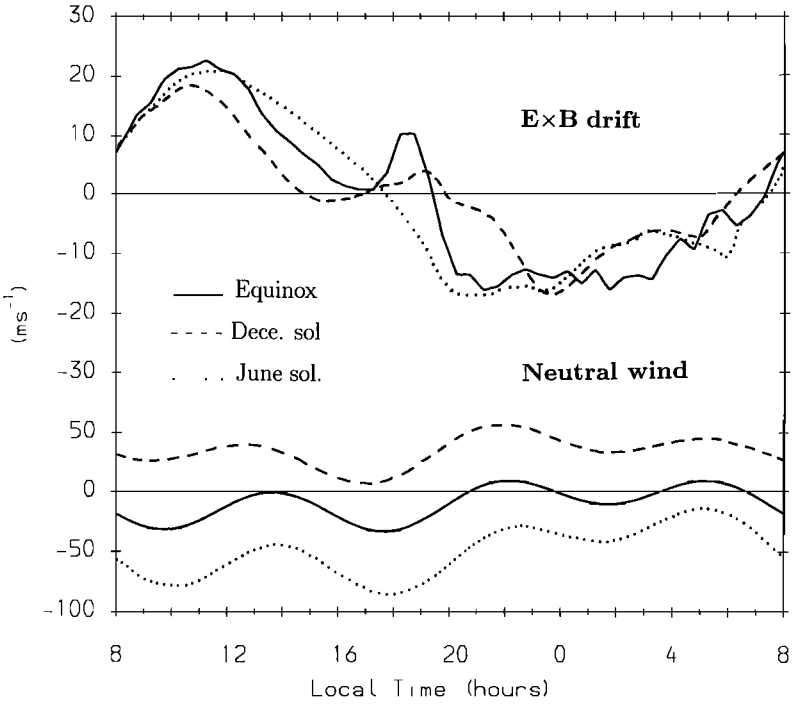

Figure 1. Local time variations of (top) the equatorial vertical $\mathbf{E}\times\mathbf{B}$ drift velocity (positive upward) used in the model calculations and (bottom) the magnetic meridional neutral wind velocity (positive equatorward) at 300 km altitude for the location of Fortaleza. The drift and wind are for low solar activity.

reasonable 24-hour distribution of model data between 150 and 2000 km altitude and ± 30° magnetic latitude.

The vertical **E×B** drift velocity and the magnetic meridional neutral wind velocity are important parameters for the formation and maintenance of the F_3 layer. The drift velocities used in the model calculations are obtained from the measurements made at Jicamarca and Arecibo (77°W). The Jicamarca drift [*Fejer et al.*, 1991] is used for magnetic field lines with apex altitude less than 450 km and the Arecibo drift [*Fejer*, 1993], scaled to the magnetic equator, is used for field lines with apex altitude greater than 2000 km; a linear interpolation is used for the field lines at intermediate apex altitudes. As Figure 1 (top) shows, the equatorial **E×B** drift velocity increases upward during the morning-noon period in all seasons; this increase is needed for the formation of the F_3 layer (see section 3). The vertical **E×B** drift velocity models available for Fortaleza [*Batista et al.*, 1996] are not used in the present study as they are only available for periods of high solar activity; the present study is mainly for periods of low solar activity to suit the observations made in 1995. The neutral wind velocities are calculated from the HWM90 neutral wind model [*Hedin et al.*, 1991]. The wind velocity in the magnetic meridian (see Figure 1, bottom) controls the location of the F_3 layer (see section 3). The concentrations and temperatures of the neutral gases, solar EUV fluxes, photoelectron heating rates, and other inputs to the model are the same as those described by *Balan et al.* [1997b].

3. Physical Mechanism and Location

A physical mechanism and the location and latitudinal extent of the F_3 layer are presented and discussed using values modeled by SUPIM for longitude 38°W (Fortaleza). The solar activity index $F10.7$ and its 81-day running mean are between 90 and 100 for the days used for low solar activity calculations, and the values for the medium and high solar activity calculations are in the ranges 145–150 and 190–200, respectively. The magnetic activity is quiet for all cases with $Ap = 4$.

3.1. Physical Mechanism

The F_3 layer arises from the daytime photochemical and dynamical processes in the equatorial F region. The model electron density (Ne) profiles shown in Figure 2 illustrate the formation and maintenance of the F_3 layer. The layer forms during the morning-noon period when the production of ionization dominates over the loss of ionization and when there is large upward flow of ionization due to the combined effect of the upward **E×B** drift and the neutral wind. Early in the morning (0800 LT), there is the usual F_2 layer. With advancing time, the layer becomes broad, much broader than at other latitudes, because of the large production and unique dynamical effects of the equatorial region. Also,

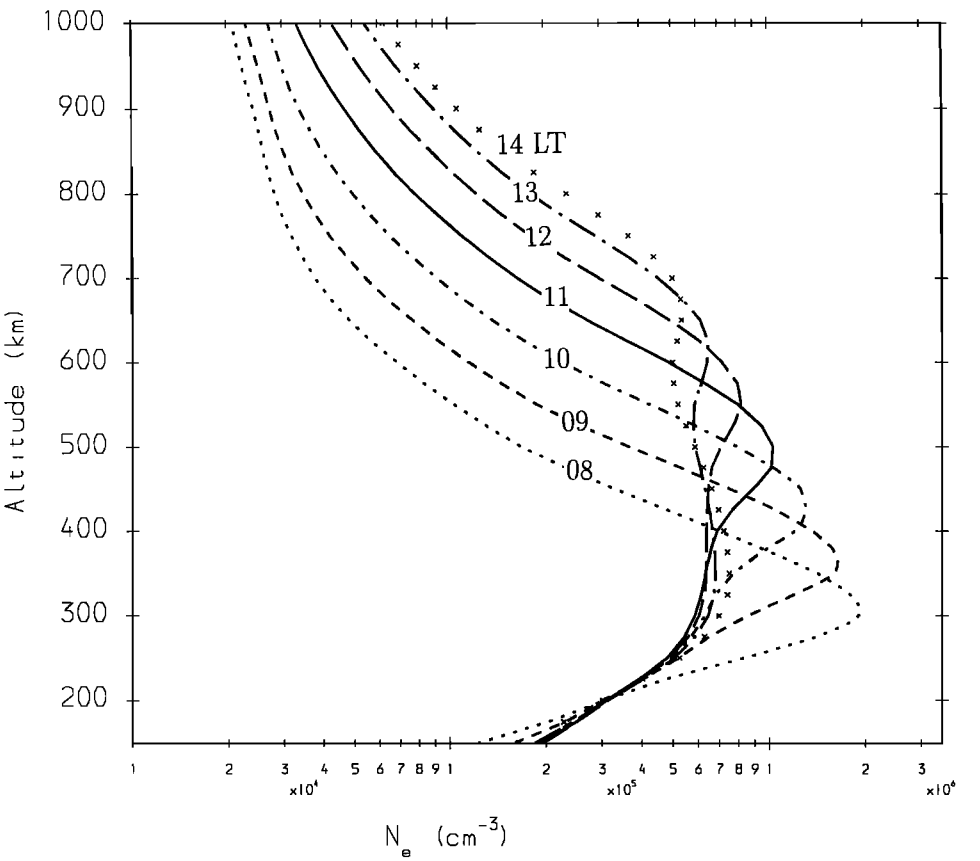

Figure 2. Model electron density profiles for the longitude of Fortaleza under conditions of strongest F_3 layer.

the peak of the layer rises in altitude, faster than at other latitudes, because of the dominating effects of the upward $\mathbf{E}\times\mathbf{B}$ drift. Until about 0930 LT, there is only a single peak. By this time the peak has risen to the top of the altitude range, where both chemical and dynamical effects are important in maintaining a single-peak layer structure; above this altitude range the dynamical effects strongly dominate the chemical effects. Thus, while the original (F_2) peak rises farther in altitude because of the dynamical effects, another peak forms at lower altitudes because of both chemical and dynamical effects. The new peak develops into the usual F_2 layer and the original (F_2) peak that drifts upward forms the F_3 layer. The two layers become distinct by about 1030 LT.

After the two layers become distinct (Figure 2) the peak electron density of the F_3 layer (N_mF_3) decreases with time, mainly because of chemical loss and diffusion (there is very little production at F_3 layer altitudes), while that of the F_2 layer (N_mF_2) increases because of production and dynamical effects. However, there is a period of time between 1030 and 1230 LT when N_mF_3 remains greater than N_mF_2. During this time both the F_2 and F_3 layers can be recorded by ground-based ionosondes as has been done at Fortaleza [*Balan et al.*, 1997b; *Jenkins et al.*, 1997]. At later times, N_mF_2 exceeds N_mF_3 and undergoes the usual daytime increase. Although N_mF_3 continues to decrease, the layer can exist until after sunset, as has been observed in the modeled and measured Ne profiles. The Ne profiles measured by the incoherent scatter radar at the equatorial station Jicamarca between 1327 and 1349 LT on January 8, 1997, show structures resembling an F_3 layer [*Aponte et al.*, 1997]. The ledges observed in the Ne profiles measured during afternoon hours at equatorial latitudes using the ISIS satellite [*Sharma and Raghavarao*, 1989] could be due to decaying F_3 layers.

Figure 2 also shows that the peak electron density (N_{max}) of the equatorial ionosphere during the morning-noon period changes from N_mF_2 to N_mF_3 and then changes back to N_mF_2. When the peak height h_{max} of the ionosphere is examined, the first changeover (N_mF_2 to N_mF_3) forms part of the morning increase of h_{max} and the second changeover (N_mF_3 to N_mF_2) produces a rapid decrease in h_{max}, which has been recorded by the ionosonde at Fortaleza [*Abdu et al.*, 1990]. The Jicamarca radar has also recorded the rapid decreases in h_{max} [*McClure et al.*, 1970; *Farley*, 1991], which have been reproduced by theoretical models [*Bailey et al.*, 1993; *Preble et al.*, 1994]. However, the decrease in h_{max} depends on the rate of decrease of N_mF_3, the rate of increase of N_mF_2, and the rate of ascent of h_mF_3 and h_mF_2. Considering the above factors, the expected decrease in h_{max} may not happen in all occurrences of an F_3 layer. Also, as seen from the model Ne profiles (Figure 2), the value of N_{max} during the morning-noon period, which includes N_mF_3 for a period of time, decreases before noon (0900–1130 LT). This does not contradict the existence of the F_3 layer, because the decrease of N_{max} is part of the noon bite-out observed at low latitudes [*Rajaram*, 1977].

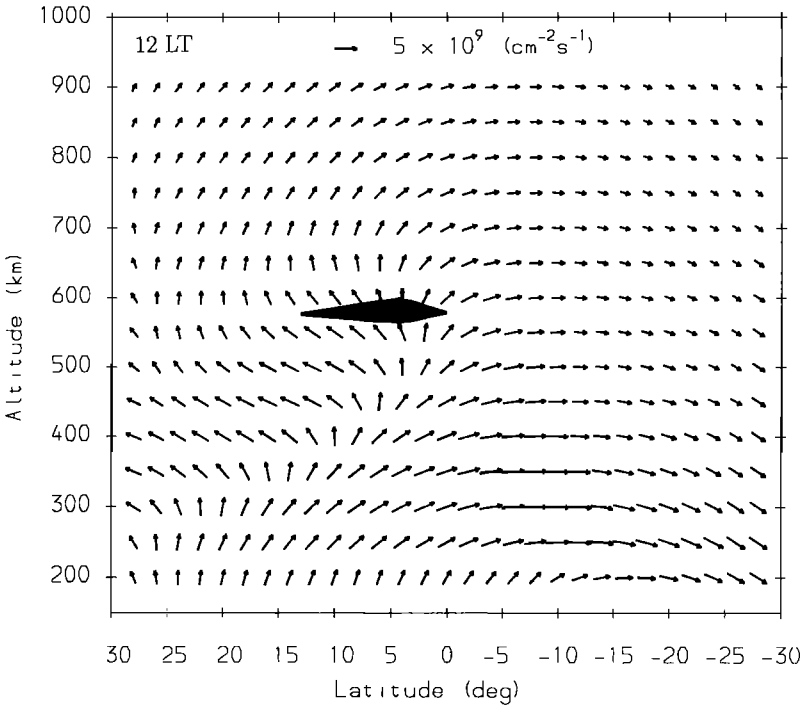

Figure 3. Vector plasma fluxes at 1200 LT which correspond to the model inputs of Figure 2. The shaded area shows the latitudinal extent of the F_3 layer, with the thick portion showing the latitude center of the layer; latitude is magnetic. The fluxes are plotted on a log scale with fluxes less than 5×10^6 cm^{-2} s^{-1} being considered to have zero length.

3.2. Location of the F_3 Layer

The F_3 layer forms near the equator and is centered at that location where there is a vertically upward plasma velocity at altitudes near and above the F_2 peak during the morning-noon period. Once formed, the layer can continue to exist provided the vertically upward plasma velocity is maintained near the altitude of the layer. This can be understood by comparing the Ne profile at 1200 LT in Figure 2 and the corresponding plasma flux vectors shown in Figure 3. The location and latitudinal extent of the F_3 layer at 1200 LT are also shown in Figure 3. The flux vectors are vertically upward at the location of the F_3 layer. A vertically upward velocity is needed because, otherwise, the plasma will diffuse downward along the geomagnetic field lines as at other latitudes; the vertical velocity should also be of sufficiently large magnitude, especially for N_mF_3 to exceed N_mF_2. The plasma velocity is determined by the resultant of the upward $\mathbf{E}\times\mathbf{B}$ drift velocity and the neutral wind velocity in the magnetic meridian. However, since the drift velocity during the morning-noon period is more or less the same for all seasons (Figure 1) and is symmetric with respect to the geomagnetic equator, the neutral wind should be the main factor in deciding the location and latitudinal extent of the F_3 layer.

An equatorward neutral wind combined with an upward $\mathbf{E}\times\mathbf{B}$ drift is needed to produce the required vertically upward plasma velocity. Considering the general circulation of the neutral wind, the F_3 layer should therefore be centered at the geomagnetic equator at the equinoxes and slightly toward the summer hemisphere at the solstices at longitudes where there is no offset in the geomagnetic and geographic equators. At other longitudes, where there is an offset in the geomagnetic and geographic equators, the layer is expected to be centered on the summer side of the geomagnetic equator at the solstices and on the side of the geomagnetic equator where there is an equatorward wind at the equinoxes. At the Brazilian longitude (38°W), where the geomagnetic equator is located on the southern side of the geographic equator, the F_3 layer is expected to be centered on the southern side of the geomagnetic equator at the December (summer) solstice and on the northern side at the June (winter) solstice; at the equinoxes the center is expected to be located at an intermediate latitude. This feature is illustrated in Figure 4, which shows the location and latitudinal extent of the F_3 layer at 1100 LT at the longitude of Fortaleza (38°W) during the solstices and equinox during low solar activity. The corresponding Ne profiles at the respective central latitudes are also shown in Figure 4. The time periods when N_mF_3 remains greater than N_mF_2 are found to be 0930–1230 LT for June solstice, 0945–1215 LT for December solstice, and 1000–1145 LT at equinox. Thus, as shown in Figure 4, a distinct F_3 layer is expected to form over Fortaleza (dip 9°S) during the December (summer) solstice; no F_3 layer is expected to form over Fortaleza at the June (winter) solstice. Figure 4 also shows that the most distinct F_3 layer at the longitude of Fortaleza is expected during the June solstice at latitudes on the northern (summer) side of the geomagnetic equator.

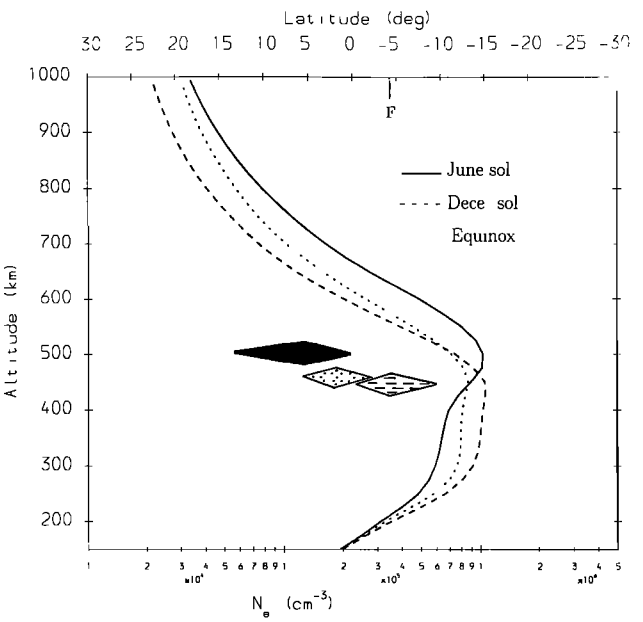

Figure 4. Latitude extent (horizontal bars) of the modeled F_3 layer at 1100 LT at the longitude of Fortaleza for December solstice, June solstice, and equinox during periods of low solar activity; the thick portion of the shaded areas correspond to the latitude centers of the layer. The electron density profiles shown correspond to the latitude centers; latitude is magnetic. The mark F denotes the location of Fortaleza.

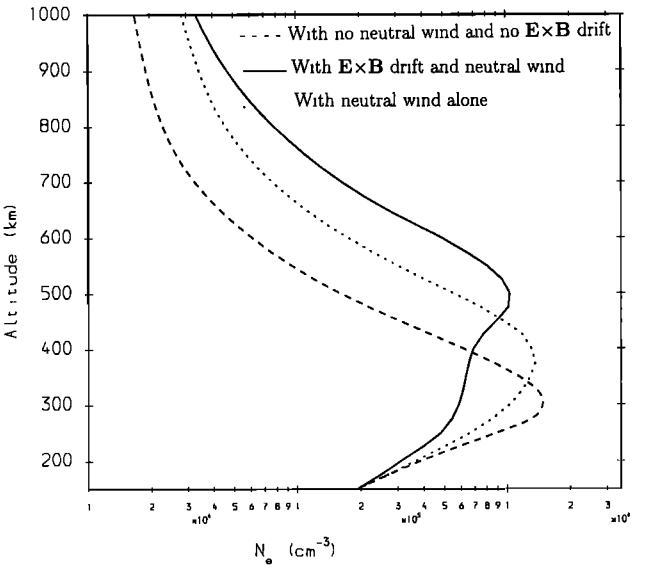

Figure 5. Electron density profiles from model calculations with no $\mathbf{E}\times\mathbf{B}$ drift and no neutral wind (dashed curve), with neutral wind and no $\mathbf{E}\times\mathbf{B}$ drift (dotted curve), and with both $\mathbf{E}\times\mathbf{B}$ drift and neutral wind (solid curve). The profiles correspond to 1100 LT at 4°N magnetic latitude at the longitude of Fortaleza during June solstice at low solar activity. Note that the F_3 layer does not form when the wind alone is used (dotted curve).

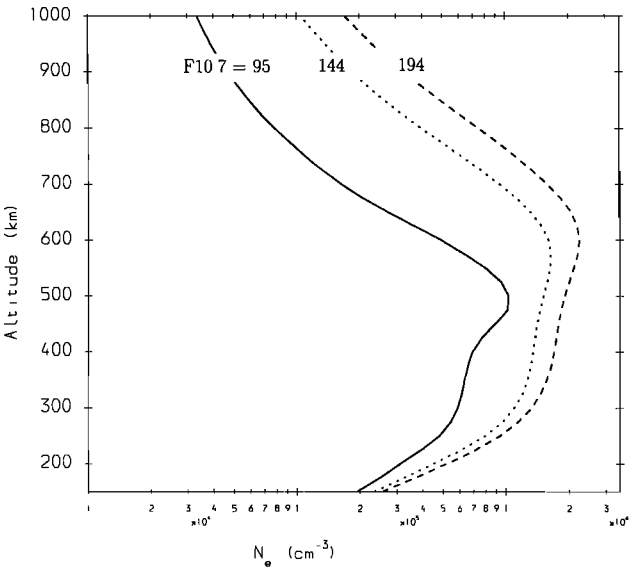

Figure 6. Electron density profiles from model calculations at the June solstice for different levels of solar activity. The profiles correspond to 1100 LT at 4°N magnetic latitude at the longitude of Fortaleza. Note that the F_3 layer becomes less distinct with increasing solar activity.

The December solstice results of *Jenkins et al.* [1997] are in agreement with those shown in Figure 4.

Although the neutral wind controls the location of the F_3 layer, the main driving force for the formation and maintenance of the F_3 layer is the upward $\mathbf{E}\times\mathbf{B}$ drift velocity. This is illustrated in Figure 5, which shows the Ne profiles modeled for different combinations of $\mathbf{E}\times\mathbf{B}$ drift and neutral wind. As Figure 5 shows, an F_3 layer forms when an $\mathbf{E}\times\mathbf{B}$ drift is included in the model calculations (solid profile); model calculations that include an $\mathbf{E}\times\mathbf{B}$ drift, but not a neutral wind, give an F_3 layer centered at the geomagnetic equator (not shown). Although the driving force (the upward $\mathbf{E}\times\mathbf{B}$ drift) undergoes a large and sudden upward strengthening during the evening hours [*Fejer et al.*, 1991], it is unlikely for an F_3 layer to form during this time. This is because during the evening period when the F_2 layer drifts upward, another layer cannot form at lower altitudes because of the absence of the production of ionization.

Figure 6 illustrates the modeled solar activity dependence of the F_3 layer. Figure 6 shows the Ne profiles at 1100 LT at 4°N magnetic latitude at the longitude of Fortaleza for different levels of solar activity at the June solstice. It can be seen that the layer for

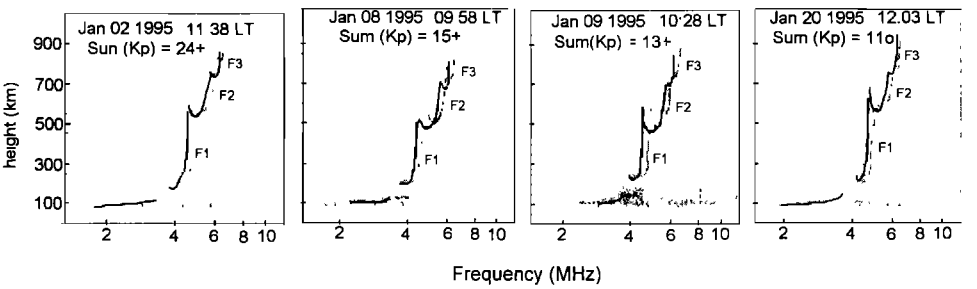

Figure 7a. Typical examples of ionograms recorded at Fortaleza during December solstice.

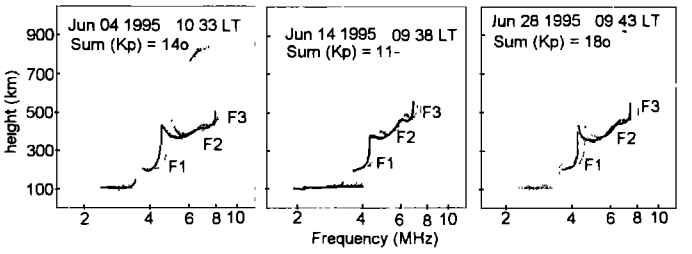

Figure 7b. Same as Figure 7a but for June solstice.

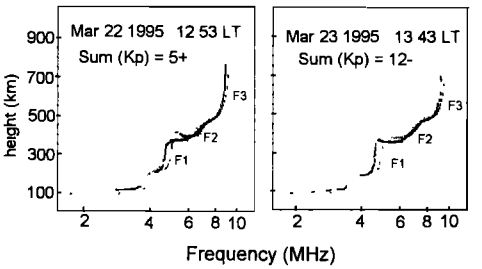

Figure 7c. Same as Figure 7a but for March equinox. Note the distinct F_3 layer trace at the December (summer) solstice compared to other seasons (Figures 7a-7c).

make the F_3 layer comparatively less distinct during medium and high solar activities is not as distinct as that for low solar activity. These differences arise because the morning-noon ionosphere becomes broad and intense with increasing solar activity, while the corresponding **E×B** drift and neutral wind remain more or less constant. Thus the upward force arising from the drift and wind becomes insufficient to raise the morning F_2 peak to the topside altitude to form a clear F_3 layer as discussed above. The greater production of ionization that results in a strong F_2 layer could also medium and high solar activities. It is to be pointed out that the above predictions on the dependence of the F_3 layer on longitude, season, and solar activity are based on the general circulation of the neutral wind as given by HWM90 and the **E×B** drift measurements made at Jicamarca.

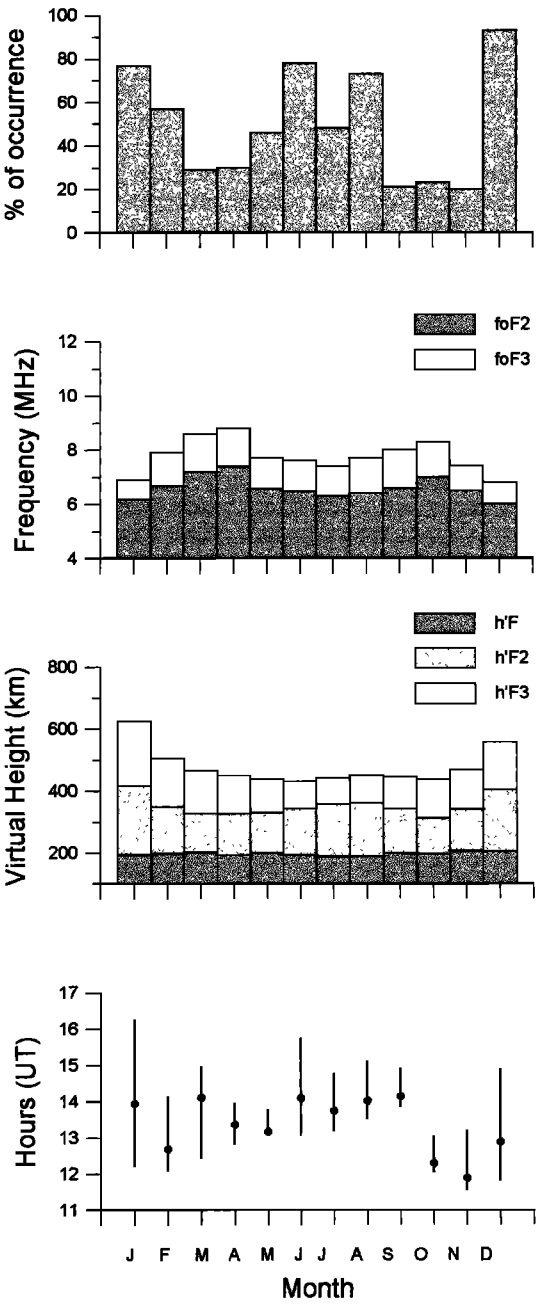

Figure 8. The frequency of occurrence, mean critical frequency, mean virtual height and mean local time duration of the F_3 layer recorded at Fortaleza for different months in 1995. The dots in the duration lines (bottom) represent the mean local time of the strongest F_3 layer; the virtual heights ($h'F$, $h'F_2$, and $h'F_3$) and critical frequency (f_0F_2 and f_0F_3) correspond to this time. Note that the F_3 layer occurs frequently at high altitudes and it lasts for the longest time in summer; the excess critical frequency of the layer compared to the F_2 layer is small in this season.

4. Statistics of Occurrence

The ionograms recorded at Fortaleza in 1995 are analyzed to study the occurrence and other characteristics of the F_3 layer; the ionograms were recorded at 5-min intervals by a digital ionosonde. On the days when the F_3 layer occurs the ionograms are found to show some distortions at the high-frequency end starting at the time when the original F_2 peak starts to form the F_3 layer. The distortions then develop into a "cusp," and an additional trace appears at the high-frequency end when the F_3 layer density exceeds the F_2 layer density. The trace lasts for a period of time (see below) and then decays and disappears. The additional trace cannot be the signature of propagating disturbances such as that caused by gravity waves for the reasons discussed by *Jenkins et al.* [1997].

Figures 7a–7c show typical examples of the ionograms displaying the F_3 layer traces recorded at Fortaleza during December solstice, June solstice, and equinox, respectively. The ionograms correspond to the local times when the F_3 layer is strongest. The daily magnetic activity index (ΣK_p) is also noted. As Figures 7a–7c show, the characteristics of the F_3 layer clearly depend on season. The layer occurs more distinctly and at higher altitudes during December solstice than during other seasons. This seasonal dependence arises because the magnetic meridional neutral wind over Fortaleza is equatorward during December (summer) solstice and poleward during other seasons (Figure 1). The equatorward wind and the upward **E×B** drift, as explained above, produce the required vertically upward plasma velocity needed to form a distinct F_3 layer during December solstice. A poleward wind, on the other hand, acts against the requirement of a vertically upward plasma velocity. The interhemispheric plasma flow from the summer hemisphere to the winter hemisphere at altitudes and latitudes outside the plasma fountain (Figure 3) also helps to form and maintain a distinct F_3 layer for a longer duration during the December (summer) solstice period.

The characteristics of the F_3 layer have been studied in detail. Figure 8 shows the frequency of occurrence and other characteristics of the F_3 layer on a monthly basis. The frequency of occurrence refers to the percentage of days of available data when f_oF_3 exceeds

f_oF_2; the data is available for almost all days except for 1 day in January and 2 days in June. It may be noted that ionosondes can detect the layer only when f_oF_3 exceeds f_oF_2. As shown by Figure 8, the layer occurs most frequently (75%) in summer (December–February) and least frequently (28%) at the equinoxes (March–May and September–November), with the occurrence in winter (June–August) falling in between (66%). The frequency of occurrence varies from a minimum of about 20% in September to a maximum of about 93% in December. The bars in the bottom of Figure 8 represent the monthly mean local time durations when the F_3 layer was recorded or when N_mF_3 exceeded N_mF_2, with the dots showing the time of strongest N_mF_3. As seen, the layer occurs earlier in the October–February period, which covers the summer season, than in other periods; the layer also lasts longest in summer. The time of occurrence varies from 0900 LT in November to 1115 LT in September, and the time duration varies from about 1 hour in October to about 4 hours in January. The altitude of the layer, shown by the mean peak virtual height ($h'F_3$, Figure 8), is also high in summer. The virtual height varies from about 430 km in June to about 625 km in January. The altitude difference between the F_3 and F_2 layers ($h'F_3$ and $h'F_2$) is also largest in summer. The base altitude of the F region ($h'F$), however, varies little on the days of the F_3 layer. Unlike the other characteristics, the critical frequency of the layer (f_0F_3) exceeds that of the F_2 layer (f_0F_2) by the largest amounts in winter and equinox (Figure 8). This is related to the winter anomaly and semiannual variation of the ionosphere, which provide more ionization in winter and equinox than in summer. The value of f_oF_3 exceeds that of f_oF_2 by a yearly average of about 1.3 MHz.

The occurrences of an F_3 layer at Fortaleza during summer (December solstice) and equinox are in general agreement with what is expected from the **E**×**B** drifts and neutral winds used in the model predictions (Figure 4). However, in winter (June solstice) when an F_3 layer is not expected to occur (Figure 4), a layer is observed almost as frequently as in summer, although for shorter durations. This could be due to the fact that (1) the upward **E**×**B** drift at Fortaleza in winter

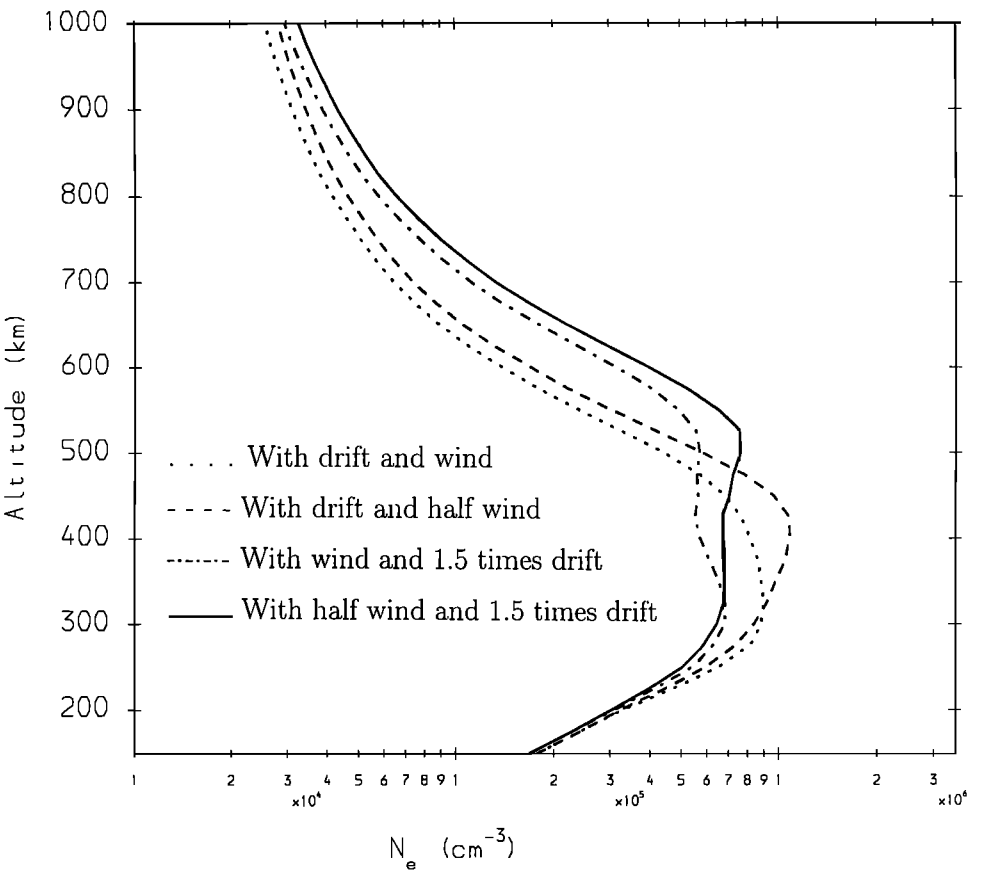

Figure 9. Electron density profiles from model calculations at 1100 LT for the location of Fortaleza at June solstice and low solar activity with (1) the daytime upward **E**×**B** drift (Figure 1) multiplied by the factor 1.5 and the neutral wind (Figure 1) unchanged (dot-dashed curve), (2) the neutral wind in the southern hemisphere multiplied by 0.5 and the drift unchanged (dashed curve), and (3) the drift multiplied by 1.5 and the wind in the southern hemisphere multiplied by 0.5 (solid curve). The profile obtained for the drift and wind shown in Figure 1 is also shown (dotted curve). Note that a combination of strong drift and weak wind can cause the occurrence of an F_3 layer at Fortaleza at the June (winter) solstice.

is stronger than that used in the calculations, or (2) the neutral wind in winter is less poleward than that given by HWM90 (Figure 1), or a combination of 1 and 2. These possibilities have been tested through model calculations. As shown by Figure 9, a combination of strong upward drift and weak poleward wind can cause the occurrence of an F_3 layer during winter. A strong upward drift and strong poleward wind can also give rise to the formation of the layer, although it cannot be recorded by ionosondes, as $N_m F_3$ remains less than $N_m F_2$. However, a weak poleward wind with a typically average drift cannot form the F_3 layer during winter.

Figures 10a–10c show the frequency of occurrence and other characteristics of the F_3 layer recorded at Fortaleza on a day-to-day basis for the months of January, June, and March, respectively. The daily magnetic

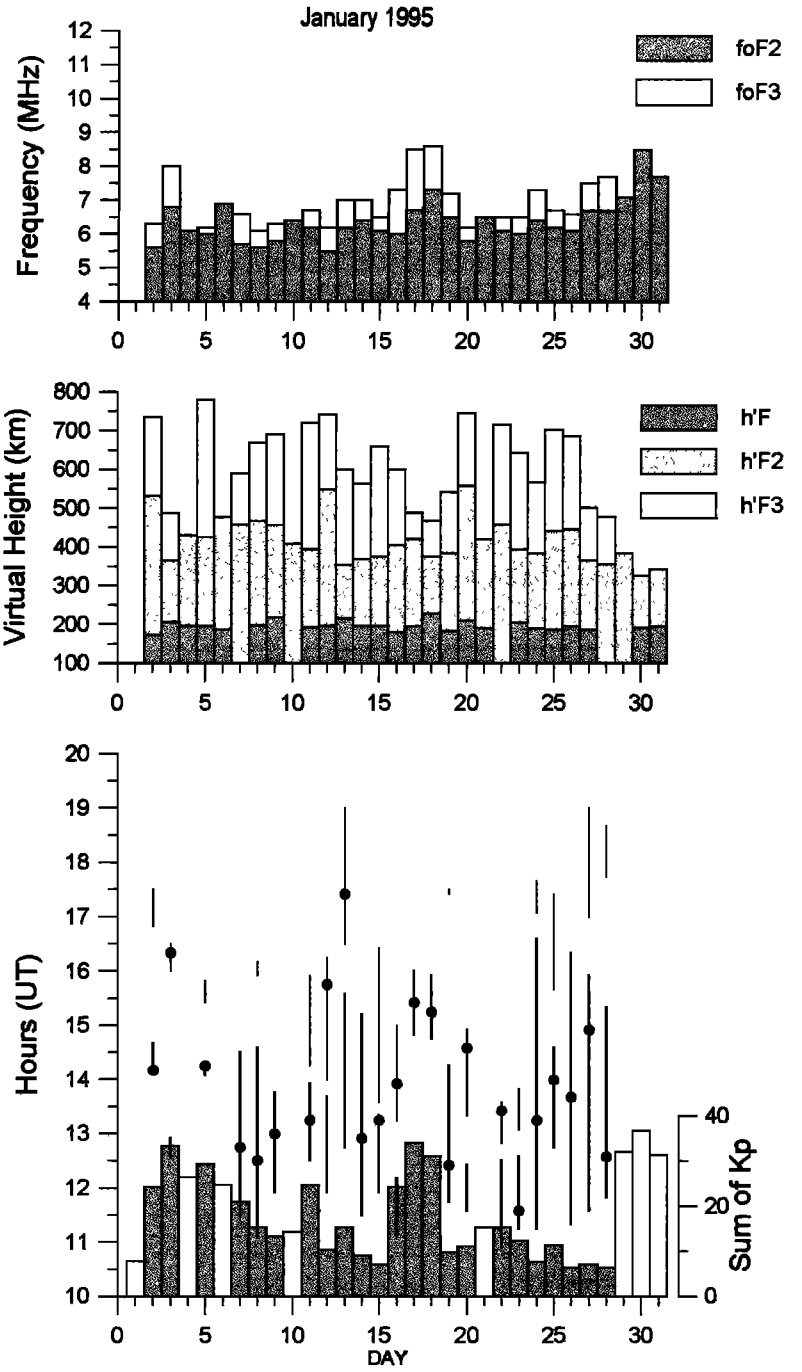

Figure 10a. The critical frequency, virtual height, local time duration (vertical lines), and frequency of occurrence of the F_3 layer recorded at Fortaleza in January 1995. The histograms at the bottom give the daily magnetic activity index ΣK_p, with the shaded histograms corresponding to the F_3 layer days. The dots in the duration lines represent the local time of the strongest F_3 layer; the virtual heights ($h'F$, $h'F_2$, and $h'F_3$) and critical frequencies (f_0F_2 and f_0F_3) correspond to this time.

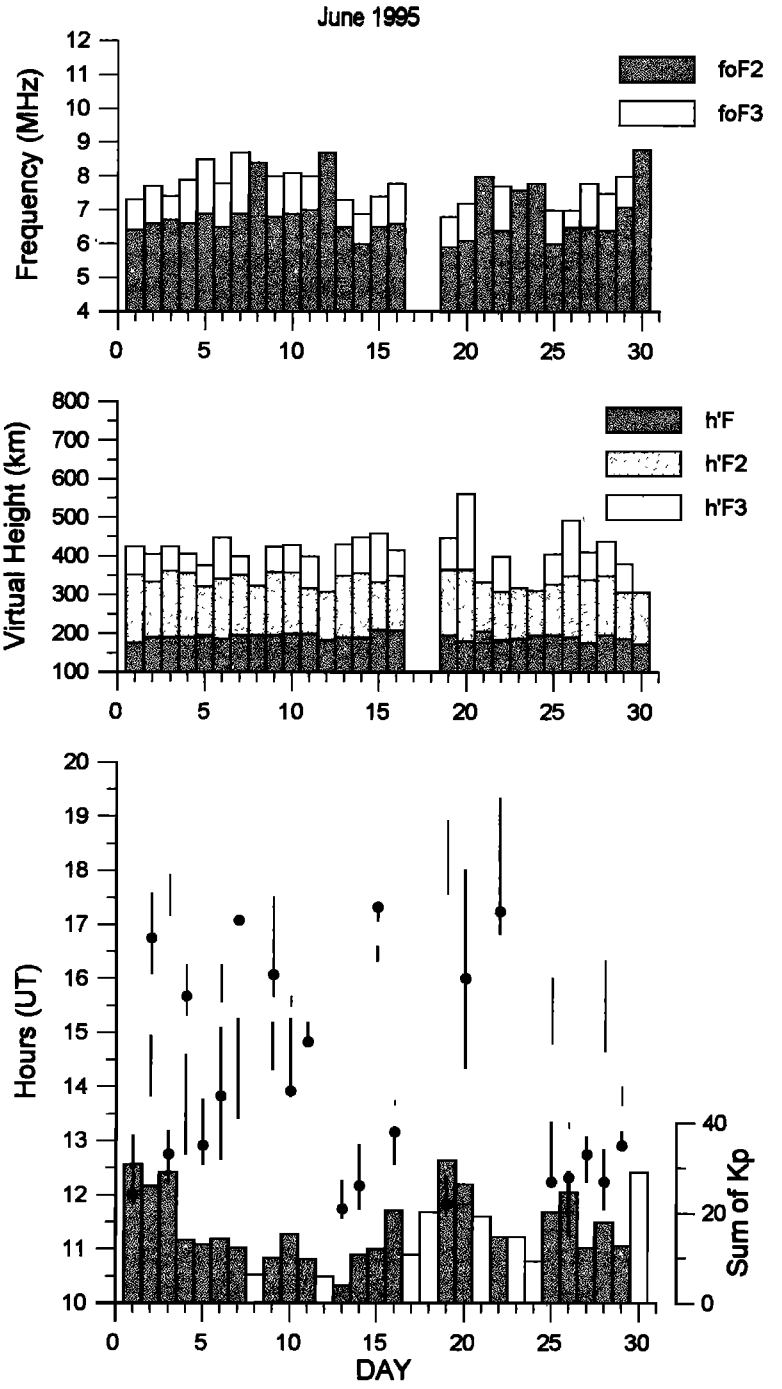

Figure 10b. Same as Figure 10a but for June 1995.

activity index (ΣK_p) is also shown as histograms, with the shaded histograms corresponding to the F_3 layer days. As Figure 10a shows, an F_3 layer occurs on 70% of the days during the summer month of January; it occurs from as early as 0900 LT and lasts from about 15 min to 5 hours (most cases last for more than 2 hours). The peak virtual height varies from about 475 to 775 km, and the critical frequency of the layer generally exceeds that of the F_2 layer by 0.2-1.0 MHz. In the winter month of June (Figure 10b) the layer occurs at a lower altitude and lasts for a shorter duration compared to the summer month (Figure 10a), although the frequency of occurrence is the same (70%). The peak virtual height in the winter month (Figure 10b) varies from about 375 to 575 km, with only one case exceeding 500 km; the duration ranges from about 15 min to 3.5 hours, with most of the cases lasting for less than 1.5 hours. Unlike the other characteristics, the critical frequency of the F_3 layer generally exceeds that of the F_2 layer by a large amount (0.5-1.8 MHz) in the winter month. This, as mentioned above, is a consequence of the winter anomaly. The frequency of occurrence (30%) and the other characteristics of the layer are small during March (equinox); see Figure 10c.

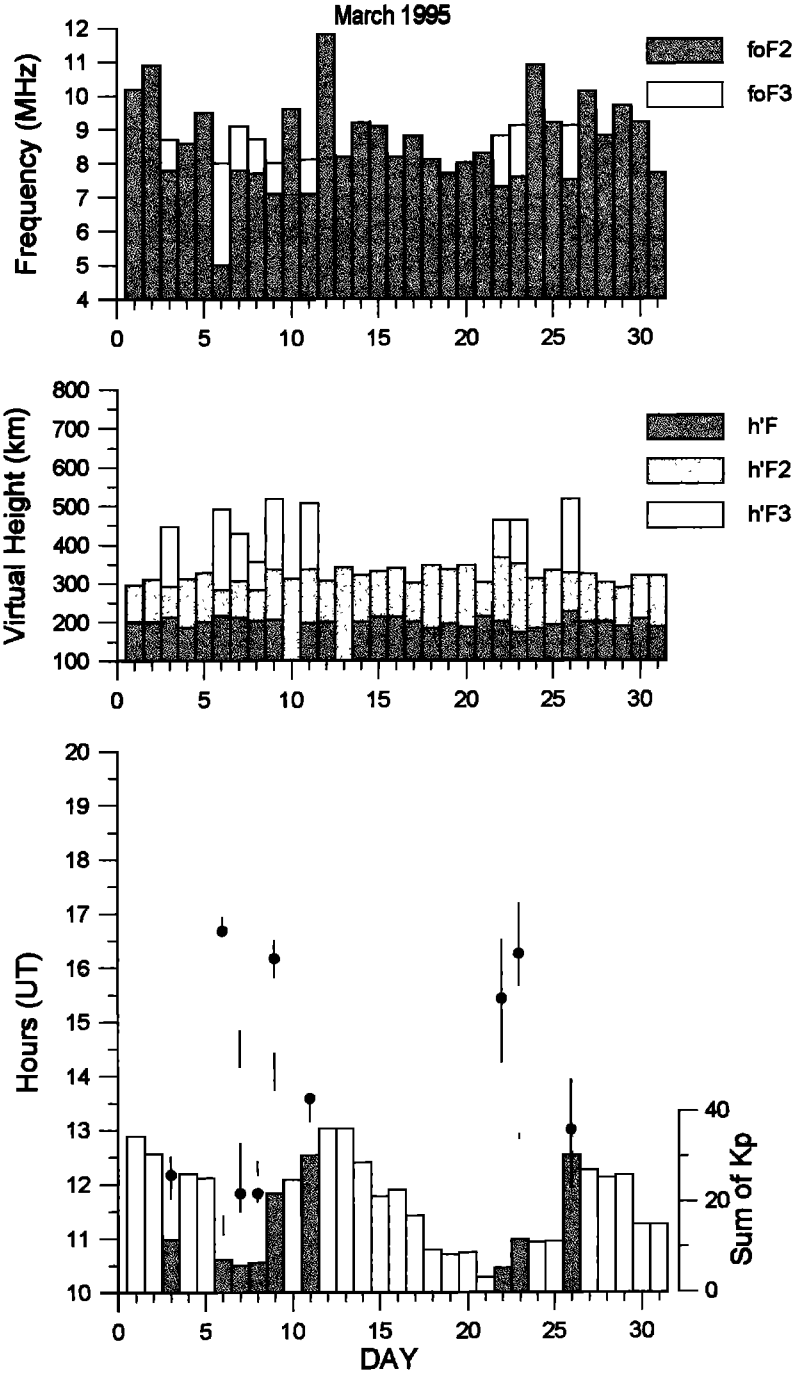

Figure 10c. Same as Figure 10a but for March 1995.

The occurrence of the layer viewed on a day-to-day basis (Figures 10a–10c) also shows that the layer occurs under both magnetically quiet and active conditions, although the occurrence is more frequent under quiet conditions. However, while the layer generally occurs during the morning hours under quiet conditions, it usually occurs in the afternoon hours under active conditions. Also, the critical frequency of the layer exceeds that of the F_2 layer by large amounts under magnetically active conditions, especially in January (Figure 10a). There is also one magnetically active period (January 29–31, 1995) when the layer did not occur (Figure 10a). The special circumstances leading to the formation of the layer under magnetically active conditions will be presented in a future paper.

The characteristics of the layer (Figures 10a–10c) show large day-to-day variability, due mainly to the day-to-day variability of the driving and modulating forces, the $\mathbf{E}\times\mathbf{B}$ drift, and the neutral wind. The variability of neutral density and solar EUV fluxes also can contribute to the variability of the layer. Also, on some days the layer reappears after disappearing. However, this is not the general case (see Figures 10a–10c). There are also successive magnetically quiet days when the layer occurs on one day and not on the other day. These special cases are being investigated.

5. Summary

Studies of the low-latitude ionosphere, using a theoretical model and experimental observations, have revealed the existence of an additional layer called the F_3 layer in the equatorial ionosphere. A physical mechanism and a study of the location and latitudinal extent of the layer for different seasons have been presented using the mathematical model SUPIM with $\mathbf{E}\times\mathbf{B}$ drift velocities measured at Jicamarca and neutral wind velocities given by HWM90. The physical mechanism holds for all longitudes, while the location and latitudinal extent are for longitude 38°W, the longitude of Fortaleza in Brazil. The statistics of occurrence of the layer recorded by an ionosonde at Fortaleza have also been presented.

The F_3 layer forms during the morning-noon period in the equatorial region where the combined effect of the upward $\mathbf{E}\times\mathbf{B}$ drift and neutral wind provides vertically upward plasma velocity at altitudes near and above the F_2 peak. The vertical velocity causes the F_2 peak to drift upward and form the F_3 layer while the normal F_2 layer develops at lower altitudes through the usual photochemical and dynamical processes of the equatorial region. The density of the F_3 layer can exceed that of the F_2 layer. The layer is predicted to be distinct and frequent on the summer side of the geomagnetic equator and to become less distinct with increasing solar activity. The latitudinal extent of the layer can extend to the winter side of the geomagnetic equator if a strong upward $\mathbf{E}\times\mathbf{B}$ drift, or a weak poleward wind, or a combination of the two, exists.

The ionograms recorded at Fortaleza in 1995 show the existence of the layer on 49% of the days, with 75% in summer, 66% in winter, and 28% in equinox. On average, the layer starts to occur at 0930 LT in summer, 1045 LT in winter, and 1015 LT in equinox and lasts for about 3.1, 1.9, and 1.2 hours, respectively. The peak (virtual) height of the layer is about 570 km in summer, 440 km in winter, and 450 km at equinox. Unlike the other characteristics, the critical frequency of the layer exceeds that of the F_2 layer by the largest amount in winter and equinox, which is related to the winter anomaly and semiannual variation of the ionosphere; f_oF_3 exceeds f_oF_2 by an yearly average of about 1.3 MHz. On a day-to-day basis the layer occurs as early as 0800 LT to as late as 1700 LT and lasts for as little as 15 min to as long as 6 hours. The peak height of the layer varies from 375 to 775 km, and the critical frequency exceeds that of the F_2 layer by 0.2-2.3 MHz.

Acknowledgments. The authors thank Y. Z. Su of the University of Sheffield for useful comments. N. Balan thanks the CNPq of Brazil for the award of a Visiting Professor fellowship.

The Editor thanks Robert Stening and David L. Hysell for their assistance in evaluating this paper.

References

Abdu, M. A., Major phenomena of the equatorial ionosphere-thermosphere system under disturbed conditions, *J. Atmos. Sol. Terr. Phys., 59,* 1505, 1997.

Abdu, M. A., R. T. De Medeiros, and J. H. A. Sobral, Equatorial spread-*F* instability conditions as determined from ionograms, *Geophys. Res. Lett., 9,* 692, 1982.

Abdu, M. A., G. O. Walker, B. M. Reddy, J. H. S. Sobral, B. G. Fejer, T. Kikuchi, N. B. Trivedi, and E. P. Szuszczewicz, Electric field versus neutral wind control of the equatorial anomaly under quiet and disturbed condition: A global perspective from SUNDIAL 86, *Ann. Geophys., 8,* 420, 1990.

Anderson, D. N., Modeling the ambient, low latitude *F* region ionosphere–A review, *J. Atmos. Terr. Phys., 43,* 753, 1981.

Aponte, N., R. F. Woodman, W. E. Swartz, and D. T. Farley, Measuring ionospheric densities, temperatures, and drift velocities simultaneously at Jicamarca, *Geophys. Res. Lett., 24,* 2941, 1997.

Appleton, E. V., Two anomalies in the ionosphere, *Nature, 157,* 691, 1946.

Bailey, G. J., and N. Balan, A low-latitude ionosphere-plasmasphere model, in *STEP Handbook,* edited by R. W. Schunk, pp. 173-206, Utah State Univ. Logan, 1996.

Bailey, G. J., R. Sellek, and Y. Rippeth, A modeling study of the equatorial topside ionosphere, *Ann. Geophys., 11,* 263, 1993.

Bailey, G. J., N. Balan, and Y. Z. Su, The Sheffield University plasmasphere ionosphere model – A review, *J. Atmos. Sol. Terr. Phys., 59,* 1541, 1997.

Balan, N., and G. J. Bailey, Equatorial plasma fountain and its effects: Possibility of an additional layer, *J. Geophys. Res., 100,* 2047, 1995.

Balan, N., K.-I. Oyama, G. J. Bailey, S. Fukao, S. Watanabe, and M. A. Abdu, A plasma temperature anomaly in the equatorial topside ionosphere, *J. Geophys. Res., 102,* 7485, 1997a.

Balan, N., G. J. Bailey, M. A. Abdu, K. I. Oyama, P. G. Richards, J. MacDougall, and I. S. Batista, Equatorial plasma fountain and its effects over three locations: Evidence for an additional layer, the F_3 layer, *J. Geophys. Res., 102,* 2047, 1997b.

Batista, I. S., T. de Medeiros, M. A. Abdu, and J. R. de Souza, Equatorial ionospheric vertical plasma drift model over the Brazilian region, *J. Geophys. Res., 101,* 10,887, 1996.

Booker, H. G., and H. W. Wells, Scattering of radio waves by the *F* region of the ionosphere, *J. Geophys. Res., 43,* 249, 1938.

Farley, D. T., Early incoherent scatter observations at Jicamarca, *J. Atmos. Terr. Phys., 53,* 665, 1991.

Fejer, B. G., *F* region plasma drifts over Arecibo: Solar cycle, seasonal, and magnetic activity effects, *J. Geophys. Res., 98,* 13,645, 1993.

Fejer, B. G., E. R. de Paula, S. A. Gonzales, and R. F. Woodman, Average vertical and zonal *F* region plasma drifts over Jicamarca, *J. Geophys. Res., 96,* 13,901, 1991.

Hanson, W. B., and R. J. Moffett, Ionization transport effects in the equatorial *F* region, *J. Geophys. Res., 71,* 5559, 1966.

Hedin, A. E., et al., Revised global model of thermosphere winds using satellite and ground-based observations, *J. Geophys. Res., 96,* 7657, 1991.

Jayachandran, B., N. Balan, P. B. Rao, J. H. Sastri, and G. J. Bailey, HF doppler and ionosonde observations on the onset conditions of equatorial spread *F*, *J. Geophys. Res., 98,* 13,741, 1993.

Jenkins, B., G. J. Bailey, M. A. Abdu, I. S. Batista, and N. Balan, Observations and model calculations of an additional layer in the topside ionosphere above Fortaleza, Brazil, *Ann. Geophys., 15,* 753, 1997.

Kelley, M. C., Equatorial spread *F*: Recent results and outstanding problems, *J. Atmos. Terr. Phys., 47,* 745, 1985.

McClure, J. P., D. T. Farley, and R. Cohen, Ionospheric electron concentration measurements at the magnetic equator, *ESSA Tech. Rep. ERL 186-AL4*, Natl. Oceanogr. and Atmos. Admin., Boulder, Colo., 1970.

Moffett, R. J., The equatorial anomaly in the electron distribution of the terrestrial *F* region, *Fundam. Cosmic Phys., 4,* 313, 1979.

Ossakow, S. L., Spread-*F* theories - A review, *J. Atmos. Terr. Phys., 43,* 437, 1981.

Oyama, K.-I., M. A. Abdu, N. Balan, G. J. Bailey, S. Watanabe, T. Takahashi, E. R. de Paula, I. S. Batista, F. Isoda, and H. Oya, High electron temperature associated with the prereversal enhancement in the equatorial ionosphere, *J. Geophys. Res., 102,* 7485, 1997.

Preble, A. J., D. N. Anderson, B. G. Fejer, and P. H. Doherty, Comparison between calculated and observed *F* region electron density profiles at Jicamarca, Peru, *Radio Sci., 29,* 857, 1994.

Rajaram, G., Structure of the equatorial *F* region, topside and bottomside–A review, *J. Atmos. Terr. Phys., 39,* 1125, 1977.

Sastri, J. H., Equatorial anomaly in *F* region – A review, *Indian J. Radio Space Phys., 19,* 225, 1990.

Sekar, R., R. Suhasini, and R. Raghavarao, Effects of vertical winds and electric fields in the nonlinear evolution of equatorial spread *F*, *J. Geophys. Res., 99,* 2205, 1994.

Sharma, P., and R. Raghavarao, Simultaneous occurrence of ionization ledge and counter electrojet in the equatorial ionosphere: Observational evidence and its implications, *Can. J. Phys., 67,* 166, 1989.

Sridharan, R., R. Sekar, and S. Gurubaran, Two-dimensional high-resolution imaging of the equatorial plasma fountain, *J. Atmos. Terr. Phys., 55,* 1661, 1993.

Stening R. J., Modeling the low-latitude *F* region, *J. Atmos. Terr. Phys., 54,* 1387, 1992.

Walker, G. O., Longitudinal structure of the *F* region equatorial anomaly - A review, *J. Atmos. Terr. Phys., 43,* 763, 1981.

Woodman, R. F., and C. La Hoz, Radar observations of *F*-region equatorial irregularities, *J. Geophys. Res., 81,* 5447, 1976.

M. A. Abdu, N. Balan, and I. S. Batista, Instituto Nacional de Pesquisas Espaciais, Divisao de Aeronomia – DAE/CEA, C.P. 515, 12.201-970, Sao Jose dos Campos – SP, Brazil (e-mail: abdu@dae.inpe.br; balan@dae.inpe.br; inez@dae.inpe.br)

G. J. Bailey, Department of Applied Mathematics, University of Sheffield, Sheffield S3 7RH, England (e-mail: G.Bailey@sheffield.ac.uk)

J. MacDougall, Department of Electrical Engineering, University of Western Ontario, London, Ontario, Canada N6A 5B9 (e-mail: macdougall@danlon.physics.uwo.ca)

(Received June 1, 1998; revised August 25, 1998; accepted August 25, 1998.)